Interaction of Naproxen with Alpha-Cyclodextrin and Its Noncyclic Analog Maltohexaose

Giampiero Bettinetti,[1,4] Milena Sorrenti,[1] Alessandra Negri,[1] Massimo Setti,[2] Paola Mura,[3] and Fabrizio Melani[3]

Received August 12, 1998; accepted February 3, 1999

Purpose. To study the effect of mechanical grinding on crystallinity changes of naproxen (NAP) in mixtures with α-cyclodextrin (αCd), amorphous αCd, and maltohexaose (M6); and the possible formation of a pseudo-inclusion complex between NAP and M6 in aqueous solution.
Methods. NAP-additive physical mixtures at 0.30, 0.18, and 0.10 mass fraction of drug were tested, after increasing grinding times, by differential scanning calorimetry (DSC) and X-ray powder diffractometry (XRD). Interaction in aqueous solution was examined by phase-solubility and fluorescence analyses supported by molecular modelling.
Results. In the mixtures with each additive the fusion enthalpy per unit mass of NAP decreased and the half width at half maximum of selected X-ray diffraction peaks of NAP increased with the progress of grinding time following the loss of crystallinity of the samples. The mechanical treatment apparently did not affect the chemical integrity of the drug. Particularly active in the equimolar mixture was the best amorphizing agent, M6. Solution studies and molecular modelling confirmed M6 may have the feature of a supermolecule for NAP, which forms a 1:1 pseudo-inclusion complex that was as stable as the true inclusion complex with αCd.
Conclusions. The intrinsically amorphous linear analog of αCd might be a potential amorphism-inducing agent and solubilizer for scarcely water soluble drugs.

KEY WORDS: naproxen; α-cyclodextrin; maltohexaose; thermal analysis; powder X-ray diffraction; molecular modelling.

INTRODUCTION

Conversion of poorly water soluble crystalline drugs into the amorphous state is a possible approach for improving the biopharmaceutical properties of solid oral dosage forms (1). Drug amorphization can be obtained by producing a molecular dispersion by grinding the drug with pharmaceutical additives (cellulose, chitin or chitosan, cyclodextrins, polyvinylpirrolidone, etc.) to an extent which generally depends on the relative amount of the additive and grinding time. Naproxen (NAP), a scarcely water soluble (about 27 mg L^{-1} at 25 °C) non-steroidal antiinflammatory drug, which is not easily transformable into the amorphous state by freeze-drying or spray-drying, can be brought to a noncrystalline state in solid combination with intrinsically amorphous additives such as randomly substituted methyl, hydroxypropyl, and hydroxyethyl derivatives of β-cyclodextrin (βCd) (2–5). Previous studies with βCd showed the physical state of the additive, crystalline, or amorphous, did not significantly influence the decrease in NAP crystallinity, which was relatively more pronounced by cogrinding with the intrinsically amorphous noncyclic analog of βCd, maltoheptaose (6). In this paper our investigations have been extended to both crystalline and amorphous α-cyclodextrin (αCd) and to maltohexaose (M6), the intrinsically amorphous linear oligomer composed of six glucose units linked by α-1,4 bonds (i.e. the noncyclic analog of αCd). Differential scanning calorimetry (DSC) supported by X-ray powder diffractometry (XRD) was used to follow the decrease in crystallinity of NAP in solid combinations with each additive with the progress of grinding time. The NAP-αCd and NAP-M6 systems were also investigated in aqueous solution by means of fluorescence spectroscopy and phase-solubility analysis supported by the molecular graphics approach. The results in terms of the extent of both amorphization and solubilization of NAP are discussed to shed light on a possible role of the cyclic structure of the additive in its interactions with the drug.

MATERIALS AND METHODS

Materials

Naproxen (NAP) purchased from Sigma Chemical Company (St. Louis, Missouri, USA) was recrystallized from ethanol. Wacker Chemie GmbH (München 70, FRG) kindly provided α-cyclodextrin (αCd, water content 7.2 ± 0.2% as mass fraction). Maltohexaose (M6) was kindly provided by Nihon Shokuhin Kako Company Ltd. (Tokyo, Japan).

Preparation of Amorphous αCd

Amorphous αCd (water content 5.1 ± 0.4% as mass fraction) was obtained from αCd by thorough grinding (2 h for 10 g sample) in a laboratory mortar grinder (Retsch, Mod. RM 0) equipped with a mortar and pestle of sintered aluminum (7).

Preparation of Drug-Additive Mixtures

Physical mixtures of NAP (75–250 μm sieve granulometric fraction) with αCd, amorphous αCd, and M6 at 0.30, 0.18, and 0.10 NAP mass fraction of were prepared by simple homogenization of the powders by turbula mixing for 10 min. The total weight of each specimen varied from 50 to 130 mg. The homogeneity of blending was checked by DSC measurements (see below) of three samples for each preparation. The physical mixtures were manually ground using an agate mortar with a pestle and the effect of mechanical treatment on drug crystallinity was evaluated by DSC and XRD after grinding times of 0, 10, 20, and 30 min. Grinding was also performed on crystals of pure NAP for control purposes. The chemical stability of NAP in the ground samples was checked by thin

[1] Dipartimento di Chimica Farmaceutica, Università di Pavia, Viale Taramelli 12, I-27100 Pavia, Italy.
[2] Dipartimento di Scienze della Terra, Università di Pavia, Via Ferrata 1, I-27100 Pavia, Italy.
[3] Dipartimento di Scienze Farmaceutiche, Università di Firenze, Via G. Capponi 9, I-50121 Firenze, Italy.
[4] To whom correspondence should be addressed. (e-mail: betti@chifar.unipv.it)

ABBREVIATIONS: NAP, naproxen; αCd, α-cyclodextrin; βCd, β-cyclodextrin; M6, maltohexaose; DSC, differential scanning calorimetry; TG, thermogravimetry; XRD, X-ray powder diffractometry; HWHM, half width at half maximum.

0724-8741/99/0500-0689$16.00/0

layer chromatography (TLC) on TLC aluminium sheets coated with silica 60 (F_{254} Merck) which were developed in a mobile phase of acetic acid:tetrathydrofuran:toluene 1:3:30 (by volume).

Thermal Analysis

Temperature and enthalpy values were measured with a METTLER STAR^e system equipped with a DSC821^e Module and a Mettler TA 4000 apparatus equipped with a DSC 25 cell using open aluminium pans at a heating rate of 10 K min^{-1} under static air atmosphere, respectively on 3–5 mg or 6–10 mg samples and in the 30–300°C or 30–180°C temperature ranges. The relative degree of crystallinity of NAP in ground samples at a prescribed grinding time (t, min) as percent of the NAP mass fraction in the starting sample, $NAP_{RDC\%(t)}$, was estimated by Eq. (1):

$$NAP_{RDC\%(t)} = \frac{\Delta H_{gr(t)}}{\Delta H_{st}} x100 \qquad (1)$$

where $\Delta H_{gr(t)}$ and ΔH_{st} are the heats of fusion of NAP calculated in the ground samples after t min of mechanical treatment and in the starting physical mixture (or pure NAP sample), respectively (8). Heat of fusion measurements were carried out in duplicate and the relative deviation standard of crystallinity data was ±6%.

X-Ray Diffraction Measurements

XRD patterns were taken with a computer-controlled Philips PW 1800/10 apparatus equipped with a specific PC-APD software. Wavelengths: $CuK_{\alpha,1}$ = 1.54060 Å; $CuK_{\alpha,2}$ = 1.54439 Å; scan range: 2–50°2θ; scan speed: 0.02°2θ s^{-1}; monochromator: graphite crystal. The relative degree of crystallinity of NAP in mixtures ground for 30 min as percent of the NAP mass fraction in the starting physical mixture, $NAP_{RDC\%(30)}$, was estimated by Eq. (2):

$$NAP_{RDC\%(30)} = \frac{HWHM_{st}}{HWHM_{gr(30)}} x100 \qquad (2)$$

where $HWHM_{st}$ and $HWHM_{gr(30)}$ are the half width at half maximum values of a selected diffraction peak of NAP in the starting physical mixture and in the corresponding mixture ground for 30 min, respectively. The strongest diffractions peaks at 19.0°2θ (011 reflection) and 6.7°2θ (100 reflection) of NAP (reference pattern No. 40–1555 (1994) of ICDD (International Centre for Diffraction Data)) were chosen. HWHM measurements were carried out in duplicate and crystallinity data (relative standard deviation ±5%) are collected in Table I.

Solubility Studies

Solubility measurements of NAP were carried out in duplicate by adding 50 mg of drug to 30 mL of water or aqueous solution of either αCd or M6 in the 5.0 to 20.0 mmol L^{-1} concentration range to a sealed glass container which was electromagnetically stirred at a constant temperature (25 ± 0.5°C) until equilibrium was achieved (72 h). An aliquot was withdrawn and the NAP concentration was determined as described previously (3,9). The apparent binding constant of the NAP-M6 complex was calculated from the slope and intercept of the straight line of the phase-solubility diagram, in terms of Eq. (3) (10).

$$K_{(1:1)} = \frac{\text{slope}}{\text{intercept}(1-\text{slope})} \qquad (3)$$

Fluorescence Spectra

Measurements were carried out using a Perkin Elmer Mod. 650-10 S spectrofluorimeter. The fluorescence intensities of the 0.03 mM NAP aqueous solution in the presence of αCd or M6 in the 2.0–5.0 mmol L^{-1} concentration ranges were measured at 25 ± 0.5°C, at excitation and emission maxima of 330 and 358 nm, respectively. The apparent binding constants of the NAP-M6 and NAP-αCd complexes were calculated by Eq. (4)

$$\frac{1-(f_0/f_m)}{C} = -K_{(1:1)} + \frac{\phi_c \varepsilon_c K_{(1:1)} f_0}{\varphi_a \varepsilon_a f_m} \qquad (4)$$

where ε_a and ε_c are the molar absorptivities of the drug and the complex at the wavelength of excitation; ϕ_a and ϕ_c are the quantum yields of the drug and the complex; f_0 and f_m are the intensities of fluorescence of NAP in the absence and in the presence of M6 at concentration C (11).

Molecular Modelling

M6 is a linear oligomer composed of six glucose units linked by α-1,4 linkages, which can be considered the noncyclic analog of αCd (i.e. the "open" αCd). Short-chain amyloses of precise chain lengths are potential supermolecules since a guest molecule can enter the intrahelical channel and form a pseudo-inclusion complex (12). M6 in particular is reported to gain in helical stability upon complexation (13). Analysis and modelling of the structures of αCd, M6, and their complexes with NAP were carried out using the INSIGHT II 95.0 program (14). NAP molecule was built-up directly using the builder routine of the INSIGHT II program. M6 molecule was built-up by opening the macrocycle of αCd, in a left-handed amylose single helix conformation similar to that of maltoheptaose (6). The molecular structure of αCd (15) was obtained from crystallographic parameters provided by the Cambridge Crystallographic Data Centre (Cambridge, Great Britain). Each structure was subjected to a simulated annealing process from 900 to 0 K (AMBER force field, DISCOVER 2.9.7 program (14), with Homans' forcefield for oligosaccharides (16)), performing iterations until the lowest-energy conformation was found.

RESULTS AND DISCUSSION

Interaction in the Solid State

The thermal behaviour of the single components is shown in Fig. 1. A sharp endothermal effect (T_{onset} = 153.4 ± 0.3°C, T_{peak} = 156.7 ± 0.4°C, fusion enthalpy 140 ± 5 J g^{-1} (4 runs)) was associated with melting of anhydrous crystals of pure NAP (Fig. 1a). Three well defined DSC endothermic effects, peaked at about 65, 98, and 120°C and due to dehydration (7.2 ± 0.2% overall mass loss by TG (3 runs)), were recorded for αCd (Fig. 1b), whilst a broad, single endotherm (5.1 ± 0.4% mass loss by TG (3 runs)) with a shoulder at about 100°C was

Table I. Effect of 30 min of Grinding on the HWHM of the Diffraction Peaks at 19.0° and 6.7° 2θ of NAP in Combinations with Crystalline αCd, Amorphous αCd, and M6 (Standard Deviations in Parentheses Refer to Last Decimal Digit)

Sample	Mass fraction of NAP	HWHM (° 2θ)				NAP crystallinity (% of NAP mass fraction)	
		19.0° 2θ		6.7° 2θ			
		Physical mix.	Ground mix.	Physical mix.	Ground mix.	19.0° 2θ	6.7° 2θ
NAP/crystalline αCd	0.30	0.34(1)	0.39(1)	0.205(6)	0.225(8)	87	91
	0.18	0.35(1)	0.37(1)	0.156(6)	0.194(7)	95	80
	0.10	0.23(1)	0.34(1)	0.164(7)	0.205(6)	68	80
NAP/amorphous αCd	0.30	0.212(7)	0.24(1)	0.157(5)	0.187(7)	88	84
	0.18	0.26(1)	0.28(1)	0.123(4)	0.171(5)	93	72
	0.10	0.225(7)	0.27(1)	0.164(6)	0.204(7)	83	80
NAP/M6	0.30	0.206(6)	0.235(8)	0.164(5)	0.21(1)	88	78
	0.10	0.172(6)	0.25(1)	0.167(6)	0.186(8)	69	90

shown by amorphous αCd (7) (Fig. 1c). M6 dehydrated similarly to amorphous αCd (7.7 ± 0.2% mass loss by TG (3 runs)) and then displayed a glass transition (17) (T_{onset} = 184.4 ± 0.3, $T_{midpoint}$ = 187.9 ± 0.2°C (3 runs)) before beginning decomposition (Fig. 1d). The results of DSC analysis of NAP-αCd, NAP-amorphous αCd and NAP-M6 combinations are presented in Fig. 2. The melting peak of NAP was substantially unaffected in its shape and area by blending with each additive, and hence, the drug maintained its original crystallinity in the physical mixtures. Drug crystallinity was also unaffected by grinding crystals of the pure drug. Instead in coground mixtures the crystallinity of NAP decreased and the relative enthalpy change with respect to the starting physical mixture was considered to be a measure of the amount of NAP transformed to a noncrystalline state by grinding (see Materials). Quantitative data for NAP crystallinity extracted from DSC curves in Figs. 1 and 2 showed less than 10% of the mass fraction of NAP was brought to a noncrystalline state in each combination with amorphous αCd, which was the poorest amorphizing agent for NAP. The intrinsically amorphous hydroxypropyl αCd MS 0.6, which has been previously tested in this respect, exhibited a more pronounced amorphizing capacity and led to 46% noncrystalline NAP by grinding under the same experimental conditions (5). Crystalline αCd was more effective than the amorphous counterpart when considering the amorphizing properties, particularly in the combinations at the lower mass fractions of drug (amorphous NAP content 10, 31, and 24%

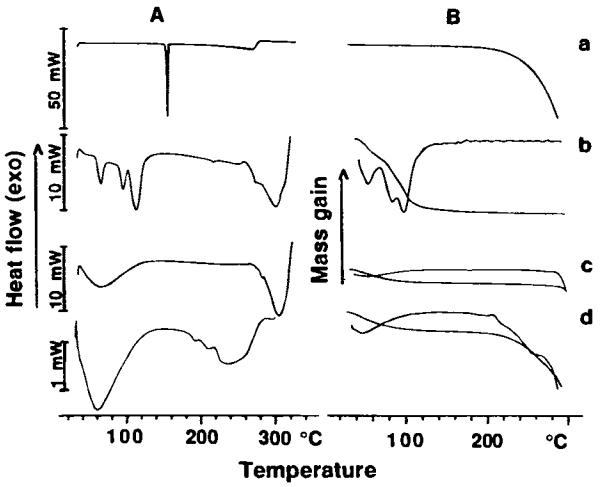

Fig. 1. DSC (A) and TG and derivative thermogravimetric (DTG) (B) curves of NAP (a), αCd (b), amorphous αCd (c), and M6 (d).

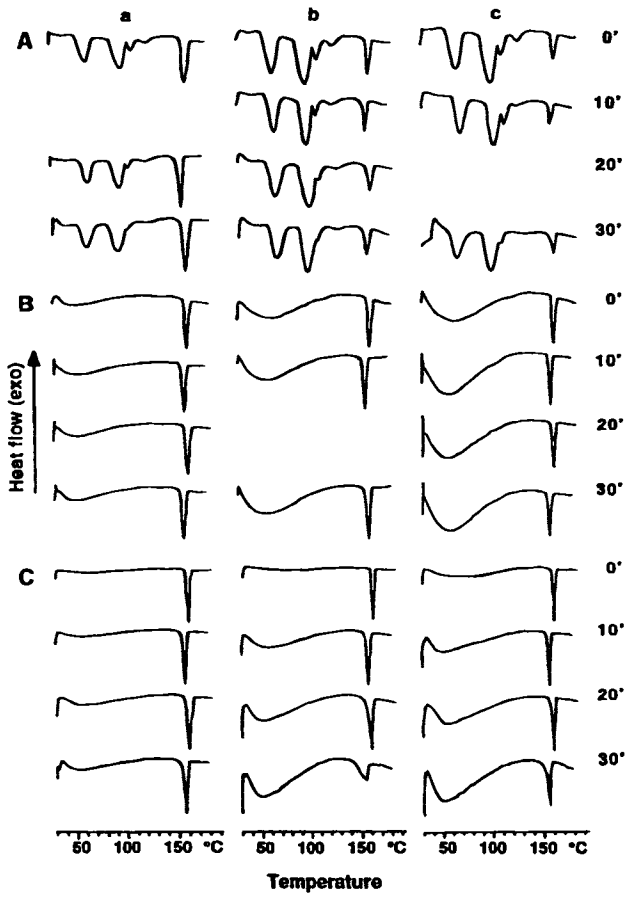

Fig. 2. DSC curves of blended and ground mixtures of NAP with αCd (A), amorphous αCd (B), and M6 (C) at 0.30 (a), 0.18 (b) and 0.10 (c) mass fractions of NAP (grinding times (min) on the curves).

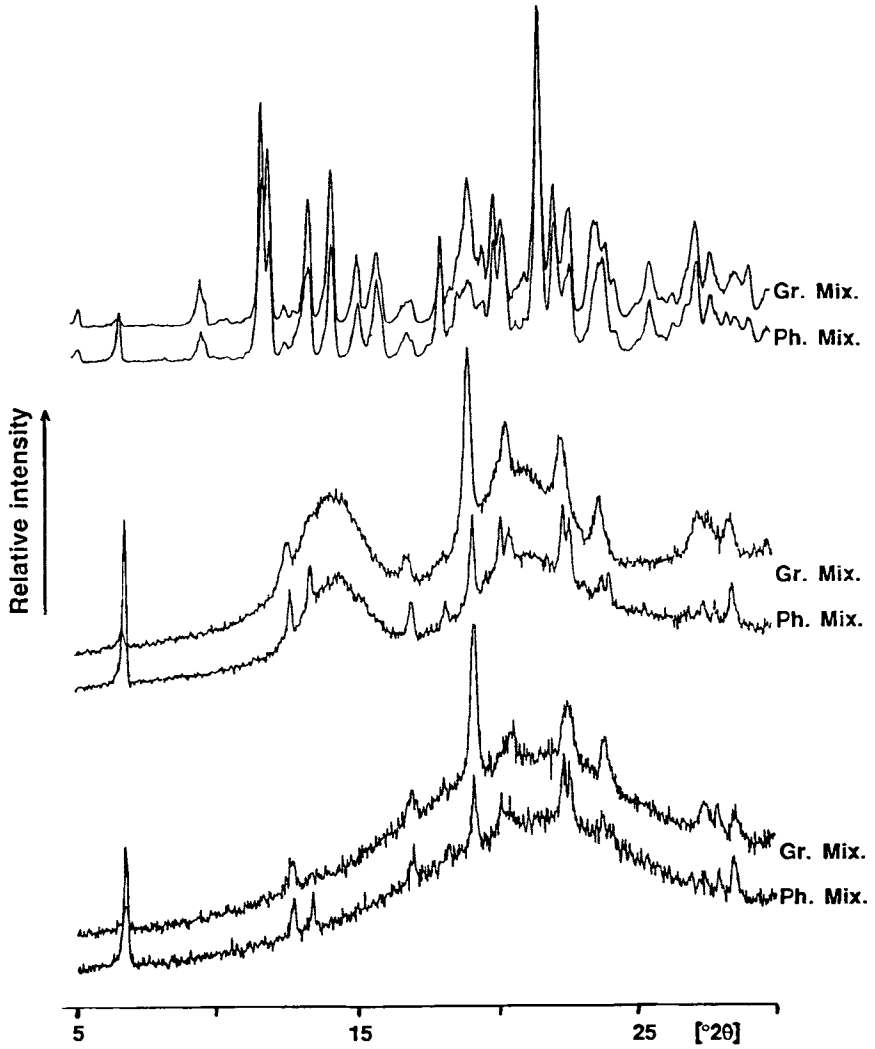

Fig. 3. X-ray powder diffraction patterns in the 5–30° 2θ range of NAP-additive (top: αCd; middle: amorphous αCd; bottom: M6) combinations at 0.10 mass fraction of NAP as physical mixtures (Ph. Mix.) and mixtures ground for 30 min (Gr. Mix.).

after 30 min of grinding in the combinations at 0.30, 0.18, and 0.10 mass fraction of NAP, respectively), but less effective than M6. Actually the amorphous NAP content after 30 min of grinding was 17, 55, and 27% in the NAP-M6 combinations respectively at 0.30, 0.18, and 0.10 mass fraction of drug. The equimolar drug-to-additive ratio was therefore the ideal composition as concerns the optimal amorphizing properties of the carrier. Maltopentaose, maltotetraose, and maltotriose (18), as well as maltoheptaose (6), showed the same feature as M6 in the respective combinations with NAP, with a linear increase in the amorphizing capacity from maltotriose to maltoheptaose. In the equimolar NAP-M6 mixture the asymmetry of the melting peak after 30 min of grinding was evident at a glance and clearly demonstrated by the lower peak onset temperature value (see Fig. 2a). Since TLC indicated each combination of the drug was not subject to chemical decomposition under the grinding conditions, this effect can be attributed to the melting of very fine NAP crystals embedded in a M6 matrix as a result of cogrinding (19).

X-ray powder diffraction patterns in the 5–30°2θ range of the NAP-additive combinations at 0.10 mass fraction of NAP (which corresponds to 0.33 mole fraction of the drug) after 0 and 30 min of grinding are shown in Fig. 3. In the NAP-amorphous αCd and NAP-M6 mixtures the diffraction peaks of NAP emerged on the diffuse background of the amorphous additive, while in the combinations with αCd also the diffraction peaks of the additive were evident. In each NAP-additive combination the decrease in crystallinity of NAP estimated by the relative broadening of the diffraction peaks at both 19.0° and 6.7°2θ after 30 min of grinding (see Materials) (Table I) was in reasonable agreement with that obtained from the relative decrease in heat of fusion. Better agreement with DSC data was shown by XRD data from HWHM measurements of the peak at 19.0°2θ for the mixtures with amorphous αCd or M6 and of the peak at 6.7°2θ for the mixtures with crystalline αCd.

Interaction in Aqueous Solution

The formation of a pseudo-inclusion compound between M6 and NAP in aqueous solution can be assumed by the A_L-type phase-solubility diagram i.e., by the linear relationship

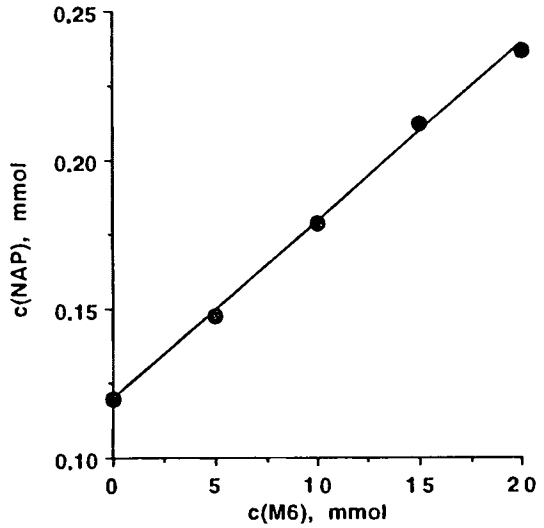

Fig. 4. Phase-solubility diagram of NAP and M6 in water at 25 °C.

between dissolved drug concentration and amount of solubilizing agent (Fig. 4). The "strength" of complexation of M6 with NAP in terms of binding constant at 25°C ($K_{1:1}$ = 49 ± 9% L mol^{-1}) was substantially the same as that of αCd ($K_{1:1}$ = 41 ± 11% L mol^{-1} (9)). Complex forming abilities of αCd > 1000- and > 4500- fold higher than those of the corresponding open form for the same guest molecule have been reported (20) and attributed to the cyclic structure which provides three-dimensional recognition of guest compound. The lipophilic cavity of αCd, which is too small to include deeply the NAP molecule and to form an equimolar inclusion complex as stable as that between NAP and αCd (21), is therefore not essential for preferential binding of NAP. The binding constant values for the NAP-αCd ($K_{1:1}$ = 83 ± 12% L mol^{-1}) and NAP-M6 ($K_{1:1}$ = 95 ± 10% L mol^{-1}) interaction obtained by fluorescence analysis (9) (Fig. 5) are very close, though binding of maltodextrins with hydrophobic fluorescence probes in water has been reported to be generally weaker and less selective

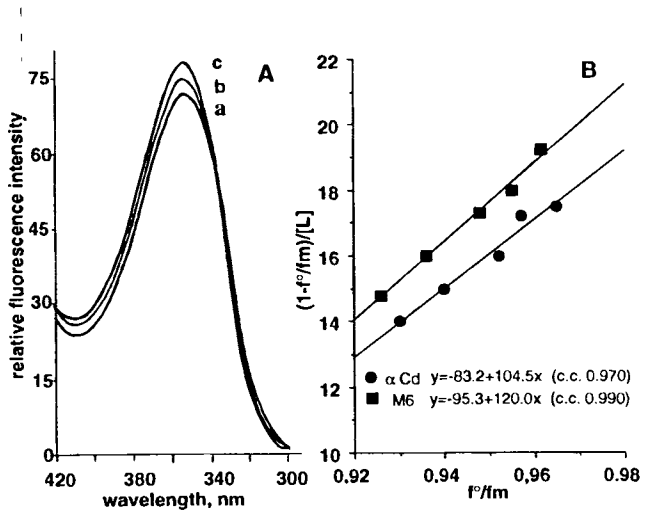

Fig. 5. A: effect of αCd and M6 on the fluorescence spectrum of 0.03 mM NAP aqueous solution (NAP alone, (a); NAP in 3.0 mM aqueous solution of αCd, (b); NAP in 3.0 mM aqueous solution of M6, (c)). B: plot derived by the Mataga-Tsuno equation (9) for NAP-αCd and NAP-M6 interactions.

than that with the preexisting cyclic counterparts (22). The results provide further experimental evidence that NAP-αCd interactions occur through insertion of a small portion of the guest into the cavity of the host (21).

Molecular modelling showed the linear analogue of αCd may have the feature of a supermolecule for NAP and accounted for the complex formed in aqueous solution, since M6 can wrap up NAP favourably taking a quasi-cyclic conformation with no large strains in the bonds between the glucoside residues (Fig. 6). Interaction energy values indicate that the NAP-M6 and NAP-αCd interactions were similar (−87.9 kJ mol^{-1} and −83.7 kJ mol^{-1} at 0 K, respectively), confirming that the "pseudo" inclusion complex of NAP with the acyclic hexamer was about as stable as the true one with the cyclic counterpart in the conformation taken from crystal structure data (23). On the other hand, the complex forming ability of M6 toward NAP in terms of interaction energy was sharply lower than that found for the higher homologue maltoheptaose (6) but distinctly higher than that of lower homologues maltopentaose, maltotetraose and maltotriose, which however still show some weak complexing properties (24). These results suggest flexible, linear maltodextrins with 3 to 7 glucose units can undergo an induced-fit type adjustment to the NAP molecule, thus providing a sort of hydrophobic environment very similar to the cavity of αCd and βCd for the terms at 6 and 7 glucose units.

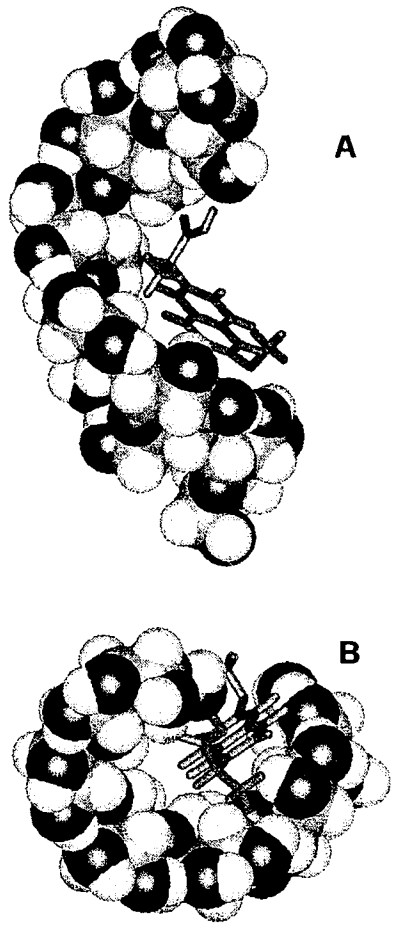

Fig. 6. Molecular model of the "pseudo" inclusion complex between NAP and M6 at 0 K: lateral view (A) and frontal view (B).

CONCLUSIONS

Malto-oligosaccharides are commonly employed as food additives, fermentation feedstocks, substrates for amylases, standards for carbohydrate analysis, etc. (25). Provided they will be available at a reasonable price, maltohexaose, maltoheptaose, and maltooctaose could be used respectively as α-, β-, and γ-cyclodextrin substitutes in the pharmaceutical applications as both solubilizing and specific amorphism-inducing agents of crystalline drugs, in case where the guest is too large to fit in the cyclodextrin cavity or the solubility of cyclodextrin is limiting. Drug-to-additive equimolar ratios are optimal in this respect and suggest a specific character of the NAP-linear maltooligomer interactions in the solid state. Cogrinding of NAP with crystalline αCd is more effective than cogrinding with αCd previously amorphized by grinding. Intrinsically amorphous hydroxypropyl αCd MS 0.6 exhibits however a more pronounced amorphizing capacity than crystalline αCd. A comparative study of the interactions of a drug with cyclodextrins and the corresponding linear maltooligomers can be of theoretical interest to support the formation of a true inclusion complex.

ACKNOWLEDGMENTS

This work was supported by a grant from Istituto Superiore di Sanità—Roma (Progetto proprietà chimico-fisiche dei medicamenti e loro sicurezza d'uso).

REFERENCES

1. B. C. Hancok and G. Zografi. Characteristics and significance of the amorphous state in pharmaceutical systems. *J. Pharm. Sci.* **86**:1–12 (1997).
2. G. P. Bettinetti, A. Gazzaniga, P. Mura, F. Giordano, and M. Setti. Thermal behaviour and dissolution properties of naproxen in combinations with chemically-modified β-cyclodextrins. *Drug. Dev. Ind. Pharm.* **18**:39–53 (1992).
3. G. P. Bettinetti, P. Mura, F. Melani, and F. Giordano. Phase-solubility analysis and molecular modelling in the study of the interaction of naproxen with hydroxyethyl β-cyclodextrins. *Proc. Int. Symp. Cyclodextrins, 7th* **1994**:455–458. Edited by T. Osa. Academic Societies Japan: Tokyo, Japan.
4. P. Mura, G. P. Bettinetti, F. Melani, and A. Manderioli. Interaction between naproxen and chemically-modified β-cyclodextrins in the liquid and solid state. *Eur. J. Pharm. Sci.* **3**:347–355 (1995).
5. F. Melani, G. P. Bettinetti, P. Mura, and A. Manderioli. Interaction of naproxen with α-, β-, and γ-hydroxypropyl cyclodextrins in solution and in the solid state. *J. Inclusion Phenom. Mol. Recognit. Chem.* **22**:131–143 (1995).
6. G. P. Bettinetti, P. Mura, F. Melani, M. Rillosi, and F. Giordano. Interactions between naproxen and maltoheptaose, the non-cyclic analog of β-cyclodextrin. *J. Inclusion Phenom. Mol. Recognit. Chem.* **25**:327–338 (1996).
7. G. P. Bettinetti, M. Rillosi, M. Setti, and P. Mura. The amorphous state of α-cyclodextrin. *Minutes Formul. Poorly-available Drugs Oral Admin.* **1996**: 311–314. Eur. Symp. (Paris). APGI. Swedish Acad. Pharm. Sciences. Ed. De Santè.
8. K. H. Kim, M. J. Frank, and N. L. Henderson. Application of differential scanning calorimetry to the study of solid drug dispersion. *J. Pharm. Sci.* **74**:283–289 (1985).
9. G. P. Bettinetti, P. Mura, A. Liguori, G. Bramanti, and F. Giordano. Solubilization and interaction of naproxen with cyclodextrins in aqueous solution and in the solid state. *Il Farmaco* **44**:195–213 (1989).
10. T. Higuchi and K. A. Connors. Phase-solubility techniques. *Adv. Anal. Chem. Instr.* **4**:117–210 (1965).
11. N. Mataga and S. Tsuno. Hydrogen bonding effect on the fluorescence of some nitrogen heterocycles. I. *Bull. Chem. Soc. Japan* **30**:368–374 (1957).
12. D. Vetter. Workshop on Supramolecular Organic Chemistry and Photochemistry, Saarbrucken (FRG), Book of Abstracts, P64 (1989).
13. D. Vetter and W. Thorn. Carbon-13 NMR spectroscopic detection of maltooligosaccharide complexes. *Starch/Staerke* **44**:271–274 (1992).
14. Biosym/MSI, 9865 Scranton Road, S. Diego, CA 92121–2777.
15. B. Klar, B. Hingerty, and W. Saenger. Topography of cyclodextrin inclusion complexes. XII. Hydrogen bonding in the crystal structure of α-cyclodextrin hexahydrate: the use of a multicounter detector in neutron diffraction. *Acta Cryst.* **B36**:1154–1165 (1980).
16. S. W. Homans. A molecular mechanic force field for the conformational analysis of oligosaccharides: comparison of theoretical and crystal structures of Man α1-3 Man β1-4 GlcNac. *Biochemistry* **29**:9110–9118 (1990).
17. P. O. Orford, R. Parker, and S. G. Ring. Aspects of the glass transition behaviour of mixtures of carbohydrates of low molecular weight. *Carbohydr. Res.* **196**:11–18 (1990).
18. M. Sorrenti, A. Negri, and G. P. Bettinetti. DSC study of crystallinity changes of naproxen in ground mixtures with linear maltooligomers. *J. Therm. Anal.* **51**:993–1000 (1998).
19. T. Oguchi, K. Terada, K. Yamamoto, and Y. Nakai. Molecular state of methyl p-hydroxybenzoate in the solid dispersion prepared by grinding with α-cyclodextrin. *Chem. Pharm. Bull.* **37**:1886–1888 (1989).
20. M. Komiyama and H. Hirai. Complex forming ability of linear glucose oligomers as non-cyclic analogs of cyclodextrins. *Makromol. Chem., Rapid Commun.* **7**:739–742 (1986).
21. G. Bettinetti, F. Melani, P. Mura, R. Monnanni, and F. Giordano. Carbon-13 nuclear magnetic resonance study of naproxen interaction with cyclodextrins in solution. *J. Pharm. Sci.* **80**:1162–1170 (1991).
22. Y. Aoyama, J. Otsuki, Y. Nagai, K. Kobayashi, and H. Toi. Host-guest complexation of oligosaccharides: interaction of maltodextrins with hydrophobic fluorescence probes in water. *Tetrahedron Lett.* **33**:3775–3778 (1992).
23. S. P. van Helden, M. J. van Drooge, A. J. Claessens, A. C. A. Jansen, and L. H. M. Janssen. A molecular modelling study of the distortion of α-cyclodextrin (cyclomaltohexaose) in complexes with guest molecules. *Carbohydr. Res.* **215**:251–260 (1991).
24. F. Melani, G. Bettinetti, P. Mura, M. Sorrenti, and A. Negri. Molecular modelling and differential scanning calorimetry studies of the interactions of naproxen with cyclodextrins and maltodextrins. *Proc. 3° Congr. Naz. Chimica Supramolecolare*, Rimini (I), 67–68 (1997).
25. A. T. Hotchkiss, Jr., R. M. Haines, and K. B. Hicks. Improved gram-quantity isolation of malto-oligosaccharides by preparative HPLC. *Carbohydr. Res.* **242**:1–9 (1993).